PERGAMON

Engineering Fracture Mechanics 69 (2002) 577–588

Engineering Fracture Mechanics

www.elsevier.com/locate/engfracmech

BEM for crack-hole problems in thermopiezoelectric materials

Qing-Hua Qin [1], Yiu-Wing Mai *

Department of Mechanical and Mechatronic Engineering J07, Centre for Advanced Materials Technology (CAMT), The University of Sydney, Sydney, NSW 2006, Australia

Abstract

The boundary element formulation for analysing interaction between a hole and multiple cracks in piezoelectric materials is presented. Using Green's function for hole problems and variational principle, a boundary element model (BEM) for a 2-D thermopiezoelectric solid with cracks and holes has been developed and used to calculate stress intensity factors of the crack-hole problem. In BEM, the boundary condition on the hole circumference is satisfied a priori by Green's function, and is not involved in the boundary element equations. The method is applicable to multiple-crack problems in both finite and infinite solids. Numerical results for stress and electric displacement intensity factors at a particular crack tip in a crack-hole system of piezoelectric materials are presented to illustrate the application of the proposed formulation.

1. Introduction

The thermoelectroelastic analysis of a multiple-crack system in a piezoelectric solid is of importance in the field of fracture mechanics, as piezoelectric materials often contain many internal microcracks which may grow during service. For anisotropic materials without thermal effect, Hwu [1] obtained a solution for collinear cracks in an infinite plate. Chen and Hasebe [2] treated the elastic interaction between a main crack and a parallel microcrack in an orthotropic plate. Based on the strain energy density criterion, Ma et al. [3] studied the direction of initial crack growth of two interacting cracks in an anisotropic solid. Mauge and Kachanov [4,5] analysed the elastic crack–microcrack interaction and the effective elastic properties of a 2-D matrix of general anisotropy, containing an arbitrary orientation distribution of cracks. Yen et al. [6] and Ting [7] obtained Green's functions for a line force and a line dislocation located outside, inside and at the interface of an elliptic inclusion of a general anisotropic elastic solid. Later, Hwu et al. [8] studied the interaction between an inclusion and a crack in an anisotropic material by the method of singular integral equations (SIE). Recently, Qin and Mai [9,10] presented thermoelectroelastic Green functions for bi-material and half-plane problems of an infinite piezoelectric solid, and applied these to obtain SIE. For a complex structure, however, the thermoelectroelastic analysis often requires more powerful numerical techniques. One such technique is the boundary element method (BEM). Most developments in fracture

* Corresponding author.
E-mail addresses: mai@aeromech.usyd.edu.au, mai@mech.eng.usyd (Y.-W. Mai).
[1] Also at Department of Mechanics, Tianjin University, China.

0013-7944/02/$ - see front matter
PII: S0013-7944(01)00095-9

mechanics by BEM can be found in Ref. [11]. In this paper, we develop a BEM for thermoelectroelastic problems of a planar piezoelectric solid with a hole and multiple cracks. Based on the thermoelectroelastic Green's function for a piezoelectric solid with a hole [12] and the potential variational principle, a system of boundary element formulation for temperature discontinuity as well as dislocation of elastic displacement and electric potential (EDEP) are presented and used to calculate stress and electric displacement (SED) intensity factors. Numerical results for a piezoelectric plate with a hole and a crack are presented to illustrate the application of the proposed method.

2. Green functions for a hole embedded in an infinite piezoelectric solid

Consider a hole embedded in an infinite piezoelectric solid subjected to a line temperature discontinuity $\widehat{T}$ located at (x_{10}, x_{20}) as shown in Fig. 1. Green functions for such a problem have been given in Ref. [12]. They are:

$$T = 2\mathrm{Re}[g'(z_t)] = 2\mathrm{Re}[f_0(\zeta_t) + f_1(\zeta_t)] \tag{1}$$

$$\vartheta = -2\mathrm{Re}[\mathrm{i}kg'(z_t)] = -2\mathrm{Re}[\mathrm{i}kf_0(\zeta_t) + \mathrm{i}kf_1(\zeta_t)] \tag{2}$$

$$\mathbf{u} = 2\mathrm{Re}\{-\mathbf{A}[\mathbf{F}_1(\zeta) + \mathbf{F}_2(\zeta)\mathbf{P}^{-1}\bar{\tau}]\mathbf{B}^{-1}\bar{\mathbf{d}} + \mathbf{c}g(\zeta_t)\} \tag{3}$$

$$\boldsymbol{\phi} = 2\mathrm{Re}\{-\mathbf{B}[\mathbf{F}_1(\zeta) + \mathbf{F}_2(\zeta)\mathbf{P}^{-1}\bar{\tau}]\mathbf{B}^{-1}\bar{\mathbf{d}} + \mathbf{d}g(\zeta_t)\} \tag{4}$$

where T, ϑ, $\mathbf{u}$ and $\boldsymbol{\phi}$ represent temperature, heat-flow function, EDEP and SED function vectors, respectively. $\mathrm{i} = \sqrt{-1}$, "Re" represents the real part of a complex number, $\zeta = \{\zeta_1\,\zeta_2\,\zeta_3\,\zeta_4\}^{\mathrm{T}}$, $\mathbf{P} = \mathrm{diag}[p_1\,p_2\,p_3\,p_4]$, τ and p_k are heat and electroelastic eigenvalues of the materials whose imaginary parts are positive [9,10]. $k = \sqrt{k_{11}k_{22} - k_{12}^2}$, where k_{ij} is the thermal conductivity, $\mathbf{A}$, $\mathbf{B}$, $\mathbf{c}$ and $\mathbf{d}$ are the material eigenvector matrices and vectors which are defined in the literature (see Refs. [9,10], for example). ζ_k and ζ_t are related to the complex variables $z_k(= x_1 + p_k x_2)$ and $z_t(= x_1 + \tau x_2)$ by, respectively

$$z_k = a(a_{1k}\zeta_k + a_{2k}\zeta_k^{-1} + e_{n1}a_{3k}\zeta_k^n + e_{n1}a_{4k}\zeta_k^{-n}) \tag{5}$$

$$z_t = a(a_{1\tau}\zeta_t + a_{2\tau}\zeta_t^{-1} + e_{n1}a_{3\tau}\zeta_t^n + e_{n1}a_{4\tau}\zeta_t^{-n}) \tag{6}$$

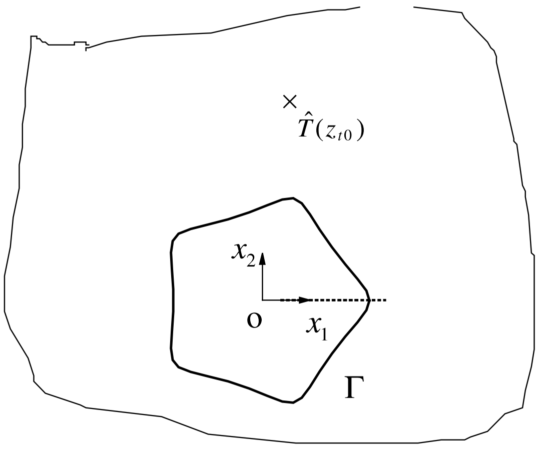

Fig. 1. Temperature discontinuity in a plate with a hole.

in which

$$a_{1k} = (1 - \mathrm{i}p_k e)/2, \quad a_{2k} = (1 + \mathrm{i}p_k e)/2, \quad a_{3k} = \gamma(1 + \mathrm{i}p_k e)/2, \quad a_{4k} = \gamma(1 - \mathrm{i}p_k e)/2 \tag{7}$$

$$a_{1\tau} = (1 - \mathrm{i}\tau e)/2, \quad a_{2\tau} = (1 + \mathrm{i}\tau e)/2, \quad a_{3\tau} = \gamma(1 + \mathrm{i}\tau e)/2, \quad a_{4\tau} = \gamma(1 - \mathrm{i}\tau e)/2 \tag{8}$$

where $e_{ij} = 1$ if $i \neq j$; $e_{ij} = 0$ if $i = j$, $0 < e \leqslant 1$, n is an integer and has the same value for both subscript and argument of the functions. γ and a are real parameters. By an appropriate selection of the parameters e, n and γ, we can obtain various kinds of cavities or holes, such as ellipse ($n = 1$), circle ($n = e = 1$), triangular ($n = 2$), square ($n = 3$) and pentagon ($n = 4$). The functions f_0, f_1, $\mathbf{F}_1$, $\mathbf{F}_2$ and g_t can be found in Ref. [12], and for convenience, we also list them in Appendix A. With the above solutions, the heat flow h_i and SED $\Pi_i(= \{\sigma_{1i}\,\sigma_{2i}\,\sigma_{3i}\,D_i\}^{\mathrm{T}})$ are calculated by the relations:

$$h_1 = -\vartheta_{,2}, \quad h_2 = \vartheta_{,1}, \quad \Pi_1 = -\phi_{,2}, \quad \Pi_2 = \phi_{,1} \tag{9}$$

where h_i, σ_{ij} and D_i are, respectively, heat flow, SED.

3. Boundary element method for thermopiezoelectric problem

Consider again a 2-D thermopiezoelectric solid inside of which there exist a hole and a number of cracks with arbitrary orientation and size. The numerical approach to such a problem usually involves the following steps. (i) Solve a heat transfer problem first to obtain the steady-state T field. (ii) Calculate the electroelastic field caused by the T field, then plus an isothermal solution to satisfy the corresponding mechanical boundary conditions. (iii) Finally, solve the modified problem for electroelastic fields. In what follows, we begin by deriving the variational principle for temperature discontinuity and then extend it to the case of thermoelectroelasticity.

3.1. Boundary element method for temperature discontinuity problem

Let us consider a finite region Ω_1 bounded by $\Gamma(= \Gamma_h + \Gamma_T)$, as shown in Fig. 2(a). The heat transfer problem to be considered is stated as:

$$k_{ij}T_{,ij} = 0 \quad \text{in } \Omega_1 \tag{10}$$

$$h_n = h_i n_i = h_0 \quad \text{on } \Gamma_h \tag{11}$$

$$T = T_0 \quad \text{on } \Gamma_T \tag{12}$$

$$h_i n_i = 0 \quad \text{on } L \tag{13}$$

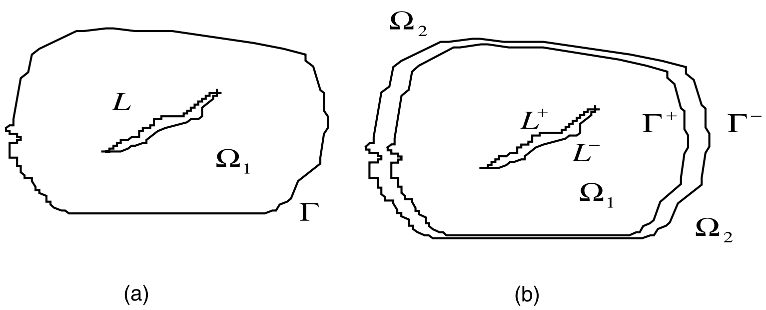

Fig. 2. Configuration of the plate for BEM analysis.

where n_i is the normal to the boundary Γ, h_0 and T_0 are the prescribed values of heat flow and temperature, which act on the boundaries Γ_h and Γ_T, respectively. For simplicity, we define $\widehat{T} = T|_{L^+} - T|_{L^-}$ on $L(= L^+ + L^-)$, where $\widehat{T}$ is the temperature discontinuity, L is the union of all cracks, L^+ and L^- are defined in Fig. 2(b). It should be pointed out that the boundary condition along the hole is automatically satisfied due to the use of the Green function given in Eqs. (1) and (2). Naturally, the hole boundary condition is not involved in the following analysis.

Further, if we let Ω_2 be the complementary region of Ω_1 (i.e., the union of Ω_1 and Ω_2 forms the infinite region Ω) and $\widehat{T} = T|_{\Gamma^+} - T|_{\Gamma^-} = T_0$, the problem shown in Fig. 2(a) can be extended to the infinite case (see Fig. 2(b)). Here $\Gamma = \Gamma^+ + \Gamma^-$, where Γ^+ and Γ^- stand for the boundaries of Ω_1 and Ω_2, respectively (see Fig. 2(b)). In a way similar to that in Ref. [13], the total generalized potential energy for the thermal problem defined above is given by:

$$P(T, \widehat{T}) = \frac{1}{2} \int_{\Omega} k_{ij} T_{,i} T_{,j} \, \mathrm{d}\Omega + \int_{\Gamma} h_n \widehat{T} \, \mathrm{d}L \tag{14}$$

By transforming the area integral in Eq. (14) to a boundary integral, we have

$$P(T, \widehat{T}) = -\frac{1}{2} \int_{L} \vartheta(T) \widehat{T}_{,s} \, \mathrm{d}s + \int_{\Gamma} h_n \widehat{T} \, \mathrm{d}s \tag{15}$$

in which the relation

$$h_i = -k_{ij} T_{,j} \quad \text{and} \quad \int_{L} h_n \widehat{T} \, \mathrm{d}s = \int_{L} [(\vartheta \widehat{T})_{,s} - \vartheta \widehat{T}_{,s}] \, \mathrm{d}s \tag{16}$$

and the temperature discontinuity is assumed to be continuous over L and zero at the ends of L. Moreover, temperature T in Eq. (15) can be expressed in terms of $\widehat{T}$ through use of Eq. (1). Therefore, the potential energy can be further written as

$$P(\widehat{T}) = -\frac{1}{2} \int_{L} \vartheta(\widehat{T}) \widehat{T}_{,s} \, \mathrm{d}s + \int_{\Gamma} h_n \widehat{T} \, \mathrm{d}s \tag{17}$$

The analytical results for the minimum of potential (17) is not, in general, possible, and therefore a numerical procedure must be used to solve the problem. As in conventional BEM, the boundaries Γ and L are divided into a series of linear boundary elements for which the temperature discontinuity may be approximated by a linear function. To illustrate this, take a particular element m, which is a line connected by nodes m and $m+1$, as an example (see Fig. 3)

$$\widehat{T}(s) = \widehat{T}_m F_m(s) + \widehat{T}_{m+1} F_{m+1}(s) \tag{18}$$

where $\widehat{T}_m$ is the temperature discontinuity at node m, and functions $F_m(s)$, $F_{m+1}(s)$ are shown in Fig. 3.

On the use of Eqs. (1), (2) and (18), the temperature and heat-flux function at point z_t are

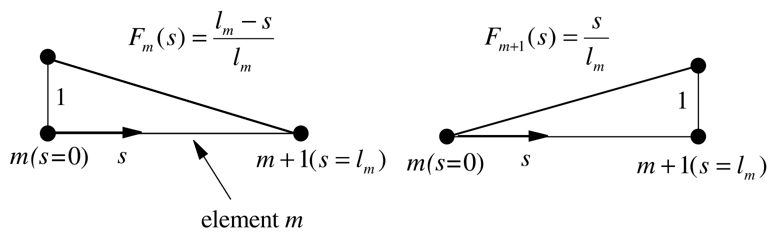

Fig. 3. The definitions of $F_m(s)$ and $F_{m+1}(s)$.

$$T(z_t) = \sum_{m=1}^{M} \mathrm{Im}[a_m(z_t)]\widehat{T}_m \tag{19}$$

$$\vartheta(z_t) = -k\sum_{m=1}^{M} \mathrm{Re}[a_m(z_t)]\widehat{T}_m \tag{20}$$

where M is the total number of nodes, "Im" represents the imaginary part of a complex number, and

$$\begin{aligned} a_m(\zeta_t) = {} & \frac{1}{2\pi}\int_{l_{m-1}} \{\ln(\zeta_t - \zeta_{t0}^{m-1}) + \ln(\zeta_t^{-1} - \bar{\zeta}_{t0}^{m-1})\}\frac{l_{m-1}-s}{l_{m-1}}\,\mathrm{d}s \\ & + \frac{1}{2\pi}\int_{l_m} \{\ln(\zeta_t - \zeta_{t0}^{m}) + \ln(\zeta_t^{-1} - \bar{\zeta}_{t0}^{m})\}\frac{s}{l_m}\,\mathrm{d}s \end{aligned} \tag{21}$$

in which ζ_{t0} can be expressed in terms of s by the relations

$$z_t = f(\zeta_t) = a(a_{1\tau}\zeta_t + a_{2\tau}\zeta_t^{-1} + e_{n1}a_{3\tau}\zeta_t^{n} + e_{n1}a_{4\tau}\zeta_t^{-n}) \tag{22}$$

$$\zeta_{t0}^{m-1} = f^{-1}(z_{t0}^{m-1}), \quad \zeta_{t0}^{m} = f^{-1}(z_{t0}^{m}) \tag{23}$$

$$z_{t0}^{m-1} = d_m + s(\cos\alpha_{m-1} + \tau\sin\alpha_{m-1}), \quad z_{t0}^{m} = d_m + s(\cos\alpha_m + \tau\sin\alpha_m) \tag{24}$$

and $d_m = x_{1m} + \tau x_{2m}$, (x_{1m}, x_{2m}) is the coordinates at node m, α_m is the angle between the element m and x_1-axis, α_{m-1} is defined similarly. It should be pointed out that the solution of ζ_{t0} in Eq. (23) is multi-valued, as there exist n-roots located outside the unit circle [14]. The root whose magnitude has a minimum value is chosen in our analysis [14].

Using Eq. (19), the temperature at node j can be written as

$$T_j(\zeta_{tj}) = \sum_{m=1}^{M} \mathrm{Im}[a_m(\zeta_{tj})]\widehat{T}_m \tag{25}$$

Substituting Eq. (18) into Eq. (17) yields

$$P(\widehat{T}) \approx \sum_{j=1}^{M}\left[\sum_{m=1}^{M}\left(-\frac{1}{2}K_{mj}\widehat{T}_m\widehat{T}_j\right) + G_j\widehat{T}_j\right] \tag{26}$$

where K_{mj} is known as the stiffness matrix and G_j the equivalent nodal heat-flux vector, which are given by:

$$K_{mj} = -\frac{k}{l_{j-1}}\int_{l_{j-1}} \mathrm{Re}[a_m(\zeta_{t0}^{j-1})]\,\mathrm{d}s + \frac{k}{l_j}\int_{l_j} \mathrm{Re}[a_m(\zeta_{t0}^{j})]\,\mathrm{d}s \tag{27}$$

$$G_j = \int_{l_{j-1}+l_j} h_{*0}F_j(s)\,\mathrm{d}s \tag{28}$$

The minimization of $P(\widehat{T})$ yields

$$\sum_{j=1}^{M} K_{mj}\widehat{T}_j = G_m \tag{29}$$

The final form of the linear equations to be solved is obtained by selecting the appropriate ones, from among Eqs. (25) and (29). Eq. (25) will be chosen for those nodes at which the temperature is prescribed, and Eq. (29) for the remaining nodes. After the nodal temperature discontinuities have been calculated, the EDEP and SED at any point in the region can be evaluated by using Eqs. (3), (4) and (9). They are

$$\mathbf{u} = \sum_{j=1}^{M} \mathbf{w}_j \widehat{T}_j, \quad \Pi_1 = \sum_{j=1}^{M} \mathbf{x}_j \widehat{T}_j, \quad \Pi_2 = \sum_{j=1}^{M} \mathbf{y}_j \widehat{T}_j \tag{30}$$

where

$$\begin{aligned} \mathbf{w}_j = & -\frac{1}{2\pi}\mathrm{Im}\left\{ \int_{l_{j-1}} [\mathbf{A}(\mathbf{F}_1(\zeta) + \mathbf{F}_2(\zeta)\mathbf{P}^{-1}\bar{\tau})\mathbf{B}^{-1}\bar{\mathbf{d}} - \mathbf{c}g(\zeta_t)] \frac{l_{j-1} - s}{l_{j-1}} \,\mathrm{d}s \right\} \\ & -\frac{1}{2\pi}\mathrm{Im}\left\{ \int_{l_j} [\mathbf{A}(\mathbf{F}_1(\zeta) + \mathbf{F}_2(\zeta)\mathbf{P}^{-1}\bar{\tau})\mathbf{B}^{-1}\bar{\mathbf{d}} - \mathbf{c}g(\zeta_t)] \frac{s}{l_j} \,\mathrm{d}s \right\} \end{aligned} \tag{31}$$

$$\begin{aligned} \mathbf{x}_j = & \frac{1}{2\pi}\mathrm{Im}\left\{ \int_{l_{j-1}} [\mathbf{B}(\mathbf{F}_1'(\zeta)\mathbf{P} + \mathbf{F}_2'(\zeta)\bar{\tau})\mathbf{B}^{-1}\bar{\mathbf{d}} - \mathbf{c}\tau g'(\zeta_t)] \frac{l_{j-1} - s}{l_{j-1}} \,\mathrm{d}s \right\} \\ & +\frac{1}{2\pi}\mathrm{Im}\left\{ \int_{l_j} [\mathbf{B}(\mathbf{F}_1'(\zeta)\mathbf{P} + \mathbf{F}_2'(\zeta)\bar{\tau})\mathbf{B}^{-1}\bar{\mathbf{d}} - \mathbf{c}\tau g'(\zeta_t)] \frac{s}{l_j} \,\mathrm{d}s \right\} \end{aligned} \tag{32}$$

$$\begin{aligned} \mathbf{y}_j = & -\frac{1}{2\pi}\mathrm{Im}\left\{ \int_{l_{j-1}} [\mathbf{B}(\mathbf{F}_1'(\zeta) + \mathbf{F}_2'(\zeta)\mathbf{P}^{-1}\bar{\tau})\mathbf{B}^{-1}\bar{\mathbf{d}} - \mathbf{c}g'(\zeta_t)] \frac{l_{j-1} - s}{l_{j-1}} \,\mathrm{d}s \right\} \\ & -\frac{1}{2\pi}\mathrm{Im}\left\{ \int_{l_j} [\mathbf{B}(\mathbf{F}_1'(\zeta) + \mathbf{F}_2'(\zeta)\mathbf{P}^{-1}\bar{\tau})\mathbf{B}^{-1}\bar{\mathbf{d}} - \mathbf{c}g'(\zeta_t)] \frac{s}{l_j} \,\mathrm{d}s \right\} \end{aligned} \tag{33}$$

Thus, the surface traction charge and EDEP induced by the temperature discontinuity are of the form

$$\mathbf{t}_n^0(s) = \Pi_i n_i = \sum_{j=1}^{M} (\mathbf{x}_j n_1 + \mathbf{y}_j n_2)\widehat{T}_j, \quad \mathbf{u}_*^0(s) = \sum_{j=1}^{M} \mathbf{w}_j(s)\widehat{T}_j \tag{34}$$

In general, $\mathbf{t}_n^0(s) \neq 0$ over Γ_t (the boundary on which SED is prescribed) and $\mathbf{u}_*^0(s) \neq 0$ over Γ_u (the boundary on which EDEP is prescribed). To satisfy the SED (or EDEP) on the corresponding boundaries, we must superpose a solution of the corresponding isothermal problem with a SED (or a EDEP) equal and opposite to those of Eq. (34). The details will be given in the following sub-section.

3.2. Boundary element method for EDEP discontinuity problem

Consider again the domain Ω_1, the governing equation and its boundary conditions are described as follows:

$$\Pi_{ij,j} = 0 \quad \text{in } \Omega_1 \tag{35}$$

$$t_{ni} = \Pi_{ij} n_j = t_i^0 - (\mathbf{t}_n^0)_i \quad \text{on } \Gamma_t \tag{36}$$

$$u_i = u_i^0 - (\mathbf{u}_*^0)_i \quad \text{on } \Gamma_u \tag{37}$$

$$t_{ni}|_{L^+} = -t_{ni}|_{L^-} = -(\mathbf{t}_n^0)_i, \quad \widehat{u}_i = u_i|_{L^+} - u_i|_{L^-} - (\mathbf{u}_*^0)_i|_{L^+} + (\mathbf{u}_*^0)_i|_{L^-} \quad \text{on } L \tag{38}$$

where Γ_t and Γ_u are the boundaries on which the prescribed values of SED t_i^0 and EDEP u_i^0 are imposed, and $\Pi_{ij} = (\Pi_j)_i$. Similarly, the total potential energy for the electroelastic problem can be given as

$$\Pi(\widehat{\mathbf{u}}) = \frac{1}{2}\int_L [\boldsymbol{\phi}(\widehat{\mathbf{u}}) \cdot \widehat{\mathbf{u}}_{,s} + 2\mathbf{t}_n^0 \cdot \widehat{\mathbf{u}}]\,\mathrm{d}s - \int_\Gamma (\mathbf{t}^0 - \mathbf{t}_n^0) \cdot \widehat{\mathbf{u}}\,\mathrm{d}s \tag{39}$$

where the elastic solutions of the functions $\boldsymbol{\phi}(\widehat{\mathbf{u}})$ and $\mathbf{u}(\widehat{\mathbf{u}})$ have been given in Ref. [14]. These solutions are

$$\mathbf{u}(\widehat{\mathbf{u}}) = \frac{1}{\pi}\mathrm{Im}[\mathbf{A}\langle \ln(\zeta_\alpha - \zeta_{\alpha 0})\rangle \mathbf{B}^{\mathrm{T}}]\widehat{\mathbf{u}} + \frac{1}{\pi}\sum_{\beta=1}^{4}\mathrm{Im}[\mathbf{A}\langle \ln(\zeta_\alpha^{-1} - \bar{\zeta}_{\beta 0})\rangle \mathbf{B}^{-1}\overline{\mathbf{B}}\mathbf{I}_\beta\overline{\mathbf{B}}^{\mathrm{T}}]\widehat{\mathbf{u}} \tag{40}$$

$$\boldsymbol{\phi}(\widehat{\mathbf{u}}) = \frac{1}{\pi}\mathrm{Im}[\mathbf{B}\langle \ln(\zeta_\alpha - \zeta_{\alpha 0})\rangle \mathbf{B}^{\mathrm{T}}]\widehat{\mathbf{u}} + \frac{1}{\pi}\sum_{\beta=1}^{4}\mathrm{Im}[\mathbf{B}\langle \ln(\zeta_\alpha^{-1} - \bar{\zeta}_{\beta 0})\rangle \mathbf{B}^{-1}\overline{\mathbf{B}}\mathbf{I}_\beta\overline{\mathbf{B}}^{\mathrm{T}}]\widehat{\mathbf{u}} \tag{41}$$

where

$$\mathbf{I}_1 = \mathrm{diag}[1,0,0,0], \quad \mathbf{I}_2 = \mathrm{diag}[0,1,0,0], \quad \mathbf{I}_3 = \mathrm{diag}[0,0,1,0], \quad \mathbf{I}_4 = \mathrm{diag}[0,0,0,1] \tag{42}$$

As before the boundaries L and Γ are divided into a series of boundary elements, for which the EDEP discontinuity may be approximated through linear interpolation as

$$\widehat{\mathbf{u}}(s) = \widehat{\mathbf{u}}_m F_m(s) + \widehat{\mathbf{u}}_{m+1}F_{m+1}(s) \tag{43}$$

With approximation (43), the EDEP and SED functions given in Eqs. (40) and (41) can now be expressed by

$$\mathbf{u}(\zeta) = \sum_{m=1}^{M}\mathrm{Im}[\mathbf{A}\mathbf{D}_m(\zeta)]\widehat{\mathbf{u}}_m, \quad \boldsymbol{\phi}(\zeta) = \sum_{m=1}^{M}\mathrm{Im}[\mathbf{B}\mathbf{D}_m(\zeta)]\widehat{\mathbf{u}}_m \tag{44}$$

where

$$\begin{aligned}\mathbf{D}_m(\zeta) = {} & \frac{1}{\pi}\int_{l_{m-1}}\left\{\langle \ln(\zeta_\alpha - \zeta_{\alpha 0}^{m-1})\rangle \mathbf{B}^{\mathrm{T}} + \sum_{\beta=1}^{4}\langle \ln(\zeta_\alpha^{-1} - \bar{\zeta}_{\beta 0}^{m-1})\rangle \mathbf{B}^{-1}\overline{\mathbf{B}}\mathbf{I}_\beta\overline{\mathbf{B}}^{\mathrm{T}}\right\}\frac{l_{m-1} - s}{l_{m-1}}\,\mathrm{d}s \\ & + \frac{1}{\pi}\int_{l_m}\left\{\langle \ln(\zeta_\alpha - \zeta_{\alpha 0}^{m})\rangle \mathbf{B}^{\mathrm{T}} + \sum_{\beta=1}^{4}\langle \ln(\zeta_\alpha^{-1} - \bar{\zeta}_{\beta 0}^{m})\rangle \mathbf{B}^{-1}\overline{\mathbf{B}}\mathbf{I}_\beta\overline{\mathbf{B}}^{\mathrm{T}}\right\}\frac{s}{l_m}\,\mathrm{d}s\end{aligned} \tag{45}$$

in which ζ_t and ζ_{t0} can be expressed in terms of s by the relations

$$z_\alpha = f(\zeta_\alpha) = a(a_{1\alpha}\zeta_\alpha + a_{2\alpha}\zeta_\alpha^{-1} + e_{n1}a_{3\alpha}\zeta_\alpha^n + e_{n1}a_{4\alpha}\zeta_\alpha^{-n}) \tag{46}$$

$$\zeta_{\alpha 0}^{m-1} = f^{-1}(z_{\alpha 0}^{m-1}), \quad \zeta_{\alpha 0}^{m} = f^{-1}(z_{\alpha 0}^{m}) \tag{47}$$

$$z_{\alpha 0}^{m-1} = d_{\alpha m} + s(\cos\alpha_{m-1} + p_\alpha \sin\alpha_{m-1}), \quad z_{\alpha 0}^{m} = d_{\alpha m} + s(\cos\alpha_m + p_\alpha\sin\alpha_m) \tag{48}$$

and $d_{\alpha m} = x_{1m} + p_\alpha x_{2m}$.

In particular the displacement at node j is given by

$$\mathbf{u}(\zeta_0^j) = \sum_{m=1}^{M}\mathrm{Im}[\mathbf{A}\mathbf{D}_m(\zeta_0^j)]\widehat{\mathbf{u}}_m \tag{49}$$

Substituting Eq. (44) into Eq. (39), we have

$$\Pi(\widehat{\mathbf{u}}) = \sum_{i=1}^{M}\left[\widehat{\mathbf{u}}_i^{\mathrm{T}} \cdot \left(\sum_{j=1}^{M}\mathbf{k}_{ij}\widehat{\mathbf{u}}_j\right)\Big/ 2 - \mathbf{g}_i\right] \tag{50}$$

where

$$\mathbf{k}_{ij} = \frac{1}{l_{j-1}} \int_{l_{j-1}} \mathrm{Im}[\mathbf{D}_i^{\mathrm{T}}(\zeta_0^{j-1})\mathbf{B}^{\mathrm{T}}]\,\mathrm{d}s - \frac{1}{l_j} \int_{l_j} \mathrm{Im}[\mathbf{D}_i^{\mathrm{T}}(\zeta_0^{j})\mathbf{B}^{\mathrm{T}}]\,\mathrm{d}s \tag{51}$$

$$\mathbf{g}_j = \int_{l_{j-1}+l_j} \mathbf{G}_j F_j(s)\,\mathrm{d}s \tag{52}$$

and $\mathbf{G}_j = -\mathbf{t}_n^0$ when node j is located at the boundary L, $\mathbf{G}_j = \mathbf{t}^0 - \mathbf{t}_n^0$ for other nodes. The minimization of Eq. (50) leads to a set of linear equations

$$\sum_{j=1}^{M} \mathbf{K}_{ij}\widehat{\mathbf{u}}_j = \mathbf{g}_i \tag{53}$$

Similarly, the final form of the linear equations to be solved is obtained by selecting the appropriate ones, from among Eqs. (49) and (53). Eq. (49) will be chosen for those nodes at which the EDEP is prescribed, and Eq. (53) for the other nodes. Once the EDEP discontinuity $\widehat{\mathbf{u}}$ has been found, the SED at any point can be expressed by

$$\Pi_1 = -\sum_{m=1}^{M} \mathrm{Im}[\mathbf{BPD}_m'(\mathbf{z})]\widehat{\mathbf{u}}_m, \quad \Pi_2 = \sum_{m=1}^{M} \mathrm{Im}[\mathbf{BD}_m'(\mathbf{z})]\widehat{\mathbf{u}}_m \tag{54}$$

Therefore the SED, Π_n, in a coordinate system local to the crack line, is given by

$$\Pi_n = \boldsymbol{\Phi}(\alpha)\{-\Pi_1 \sin\alpha + \Pi_2 \cos\alpha\}^{\mathrm{T}} \tag{55}$$

where $\boldsymbol{\Phi}(\alpha)$ is defined by [14]

$$\boldsymbol{\Phi}(\alpha) = \begin{bmatrix} \cos\alpha & \sin\alpha & 0 & 0 \\ -\sin\alpha & \cos\alpha & 0 & 0 \\ 0 & 0 & 1 & 0 \\ 0 & 0 & 0 & 1 \end{bmatrix} \tag{56}$$

Using Eq. (55) we can evaluate the SED intensity factors by the following definition:

$$\mathbf{K}(c) = \{K_{II}\, K_I\, K_{III}\, K_D\}^{\mathrm{T}} = \lim_{r\to 0} \sqrt{2\pi r}\,\Pi_n(r) \tag{57}$$

We can evaluate the SED intensity factors in several ways: by extrapolation, traction and J-integral formulae [15]. In our analysis, the first method is used to calculate the SED intensity factors in BEM. Here, Π_n at points A and B ahead of a crack tip (see Fig. 4) is first derived and then substituting them into Eq. (57), we obtain

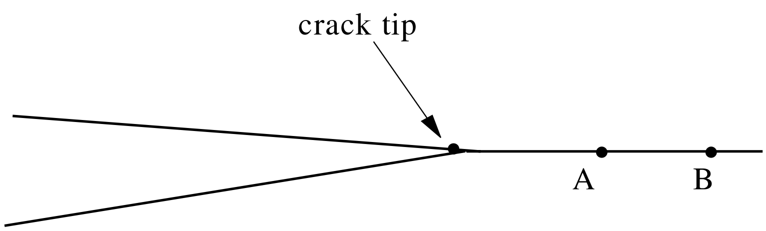

Fig. 4. Geometry of near-tip points A and B.

$$\mathbf{K}^{\mathrm{A}} = \sigma_n^{\mathrm{A}}\sqrt{2\pi r_{\mathrm{A}}}, \quad \mathbf{K}^{\mathrm{B}} = \sigma_n^{\mathrm{B}}\sqrt{2\pi r_{\mathrm{B}}} \tag{58}$$

where r_{A} (or r_{B}) are the distance from crack tip to point A (or B). Finally, the SED intensity factors $\mathbf{K}$ can be obtained by the linear extrapolation of $\mathbf{K}^{\mathrm{A}}$ and $\mathbf{K}^{\mathrm{B}}$ to the crack tip, that is

$$\mathbf{K} = \mathbf{K}^{\mathrm{A}} - \frac{\mathbf{K}^{\mathrm{B}} - \mathbf{K}^{\mathrm{A}}}{r_{\mathrm{B}} - r_{\mathrm{A}}} r_{\mathrm{A}} \tag{59}$$

4. Numerical results

Since the main purpose of this paper is to outline the basic principles of the proposed method, the numerical assessment is limited to an infinite thermopiezoelectric material containing an elliptic hole and a crack as shown in Fig. 5, in which $x_{10} = 0$, $x_{20} = 2b$ and $c = 0.5b$. The uniform heat flow h_0 is applied on each crack face only. The material is assumed to be $BaTiO_3$, whose constants are [14]

$$c_{11} = 150\ \mathrm{GPa}, \quad c_{12} = 66\ \mathrm{GPa}, \quad c_{13} = 66\ \mathrm{GPa}, \quad c_{33} = 146\ \mathrm{GPa}, \quad c_{44} = 44\ \mathrm{GPa},$$

$$\alpha_{11} = 8.53 \times 10^{-6}\ \mathrm{K}^{-1}, \quad \alpha_{33} = 1.99 \times 10^{-6}\ \mathrm{K}^{-1}, \quad \lambda_3 = 0.133 \times 10^5\ \mathrm{N/CK},$$

$$e_{31} = -4.35\ \mathrm{C/m^2}, \quad e_{33} = 17.5\ \mathrm{C/m^2}, \quad e_{15} = 11.4\ \mathrm{C/m^2}, \quad \kappa_{11} = 1115\kappa_0, \quad \kappa_{33} = 1260\kappa_0,$$

$$\kappa_0 = 8.85 \times 10^{-12}\ \mathrm{C^2/N\,m^2} = \text{permitivity of free space.}$$

In our analysis, plane strain deformation is assumed and the cracks are assumed to be in the x_1–x_2 plane, i.e., $D_3 = u_3 = 0$. Therefore the stress intensity factor vector $\mathbf{K}^*$ has only three components (K_I, K_{II}, K_D). In all calculations, $r_{\mathrm{A}} = l/7$ and $r_{\mathrm{B}} = l/5$ have been used, where l is the length in the related element. Four meshes ($N = 10$, 20, 40 and 80 elements) for the crack have been used to study the convergence of the BEM results, in which N represents the element number of the crack. In Fig. 6 the coefficients of SED intensity factors β_i at point B (see Fig. 5) are presented as a function of crack orientation angle α for $N = 80$, where β_i are defined by [14]

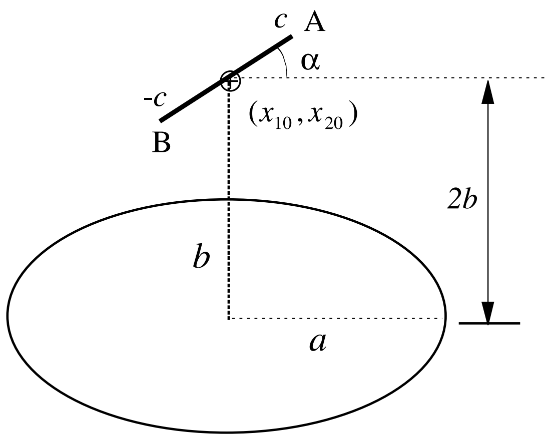

Fig. 5. Geometry of the crack-hole system.

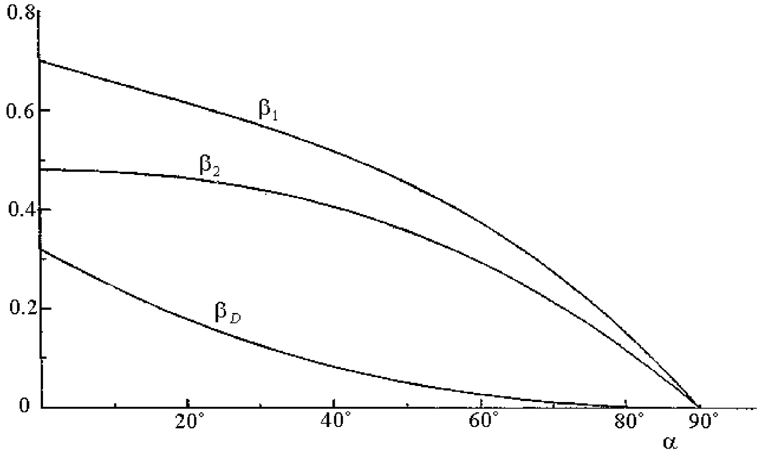

Fig. 6. SED intensity factors versus crack angle.

Table 1
SED intensity factors versus mesh refinement

Mesh ($N =$)	β_1	β_2	β_D
10	0.6969	0.4697	0.3188
20	0.6990	0.4722	0.3205
40	0.7011	0.4743	0.3223
80	0.7021	0.4752	0.3231

$$\begin{aligned} K_I(A) &= h_0 c \gamma_{33} \beta_1(\alpha) \sqrt{\pi c}/k \\ K_{III}(A) &= h_0 c \gamma_{11} \beta_2(\alpha) \sqrt{\pi c}/k \\ K_D(A) &= h_0 c \chi_3 \beta_D(\alpha) \sqrt{\pi c}/k \end{aligned} \tag{60}$$

Table 1 shows the results of SED intensity factors at point B versus mesh refinement for $\alpha = 0$. It is found from Fig. 6 that the SED intensity factors are sensitive to the crack orientation in this example. It is also found from Table 1 that the BEM results can converge to a particular value along with mesh refinement.

5. Conclusion

This study presented a boundary element formulation for the crack-hole problem of a thermopiezoelectric plate. A system of boundary element equations is developed with the aid of Green's function approach and variational principle. Solutions for the thermal, electric and elastic fields are then obtained for the crack-hole system in a piezoelectric plate under external heat-flux disturbances. For an infinite plate with a hole and a crack, the numerical results show that the crack angle α has a strong effect on the SED intensity factors. Moreover, it is obvious that there are two independent unknowns ($T^+(P)$ and $T^-(P)$ for temperature or $\mathbf{u}^+(P)$ and $\mathbf{u}^-(P)$ for displacements) at any point P on crack faces. However, the conventional boundary element formulation can generally provide one equation at each point only. The present method can bypass this problem by combining the above two unknowns into one variable ($\widehat{T}(P) = T^+(P) - T^-(P)$ for temperature field and $\widehat{\mathbf{u}}(P) = \mathbf{u}^+(P) - \mathbf{u}^-(P)$ for displacement field).

Acknowledgements

The authors wish to thank the Australian Research Council for supporting this work. Q.-H. Qin was also in receipt of an ARC Queen Elizabeth II Research Fellowship.

Appendix A

The expressions of f_0, f_1, $\mathbf{f}_1$, $\mathbf{f}_2$ and g_t in Eqs. (1)–(4)

$$f_0(\zeta_t) = \frac{\widehat{T}}{4\pi \mathrm{i}} \ln(\zeta_t - \zeta_{t0}) \tag{A.1}$$

$$f_1(\zeta_t) = -\frac{\widehat{T}}{4\pi \mathrm{i}} \ln(\zeta_t^{-1} - \bar{\zeta}_{t0}) \tag{A.2}$$

$$\mathbf{f}_i(\zeta) = \mathrm{diag}[f_i(\zeta_1) f_i(\zeta_2) f_i(\zeta_3) f_i(\zeta_4)] \quad (i = 1, 2) \tag{A.3}$$

$$\begin{aligned} g(\zeta_t) = \frac{a\widehat{T}}{4\pi \mathrm{i}} \{ & a_{1\tau}[F_1(\zeta_t, \zeta_{t0}) - F_2(\zeta_t^{-1}, \bar{\zeta}_{t0})] + a_{2\tau}[F_2(\zeta_t, \zeta_{t0}) - F_1(\zeta_t^{-1}, \bar{\zeta}_{t0})] + e_{j1} a_{3\tau}[F_3(\zeta_t, \zeta_{t0}) - F_4(\zeta_t^{-1}, \bar{\zeta}_{t0})] \\ & + a_{4\tau}[F_4(\zeta_t, \zeta_{t0}) - F_3(\zeta_t^{-1}, \bar{\zeta}_{t0})]\} \end{aligned} \tag{A.4}$$

where

$$\begin{aligned} f_1(\zeta_k) = \frac{a\widehat{T}}{8\pi \mathrm{i}} \{ & [F_1(\zeta_k, \zeta_{t0}) + F_2(\zeta, \zeta_{t0}) - F_1(\zeta_k^{-1}, \bar{\zeta}_{t0}) - F_2(\zeta_k^{-1}, \bar{\zeta}_{t0})] \\ & + e_{j1}\gamma[F_3(\zeta_k, \zeta_{t0}) + F_4(\zeta_k, \zeta_{t0}) - F_3(\zeta_k^{-1}, \bar{\zeta}_{t0}) - F_4(\zeta_k^{-1}, \bar{\zeta}_{t0})]\} \end{aligned} \tag{A.5}$$

$$\begin{aligned} f_2(z_k) = \frac{p_k a e}{8\pi} & [-F_1(\zeta_k, \zeta_{t0}) + F_2(\zeta_k, \zeta_{t0}) - F_1(\zeta_k^{-1}, \bar{\zeta}_{t0}) + F_2(\zeta_k^{-1}, \bar{\zeta}_{t0})] \\ & + e_{j1}\gamma[F_3(\zeta_k, \zeta_{t0}) - F_4(\zeta_k, \zeta_{t0}) + F_3(\zeta_k^{-1}, \bar{\zeta}_{t0}) - F_4(\zeta_k^{-1}, \bar{\zeta}_{t0})]\} \end{aligned} \tag{A.6}$$

$$F_1(\zeta_t, \zeta_{t0}) = (\zeta_t - \zeta_{t0})[\ln(\zeta_t - \zeta_{t0}) - 1] \tag{A.7}$$

$$F_2(\zeta_t, \zeta_{t0}) = (\zeta_t^{-1} - \zeta_{t0}^{-1}) \ln(\zeta_t - \zeta_{t0}) + \zeta_{t0}^{-1} \ln \zeta_t \tag{A.8}$$

$$F_3(\zeta_t, \zeta_{t0}) = (\zeta_t^m - \zeta_{t0}^m) \ln(\zeta_t - \zeta_{t0}) - \zeta_{t0}^m \sum_{n=1}^{m} \frac{1}{n} \left(\frac{\zeta_t}{\zeta_{t0}} \right)^n \tag{A.9}$$

$$F_4(\zeta_t, \zeta_{t0}) = (\zeta_t^{-m} - \zeta_{t0}^{-m}) \ln(\zeta_t - \zeta_{t0}) + \zeta_{t0}^{-m} \ln \zeta_t - \zeta_{t0}^{-m} \sum_{n=1}^{m-1} \frac{1}{n} \left(\frac{\zeta_{t0}}{\zeta_t} \right)^n. \tag{A.10}$$

References

[1] Hwu C. Collinear cracks in anisotropic bodies. Int J Frac 1991;52:239–56.
[2] Chen YH, Hasebe N. Interaction between a main-crack and a parallel micro-crack in an orthotropic plane elastic solid. Int J Solids Struct 1994;31:1877–90.
[3] Ma H, Zhao LG, Chen YH. Crack initiation angles for systems of two interacting cracks in media with rectilinear preferred directions. Theor Appl Frac Mech 1996;24:253–61.

[4] Mauge C, Kachanov M. Anisotropic material with interacting arbitrarily oriented cracks: Stress intensity factors and crack–microcrack interactions. Int J Frac 1994;65:115–39.
[5] Mauge C, Kachanov M. Effective elastic properties of an anisotropic material with arbitrarily oriented interacting cracks. J Mech Phys Solids 1994;42:561–84.
[6] Yen WJ, Hwu C, Liang YK. Dislocation inside, outside or on the interface of an anisotropic elliptical inclusion. J Appl Mech 1995;62:306–11.
[7] Ting TCT. Green's functions for an anisotropic elliptic inclusion under generalized plane strain deformations. Q J Mech Appl Math 1996;49:1–18.
[8] Hwu C, Liang YK, Yen WJ. Interactions between inclusions and various types of cracks. Int J Frac 1995;73:301–23.
[9] Qin QH, Mai YW. Crack growth prediction of an inclined crack in a half-plane thermopiezoelectric solid. Theor Appl Frac Mech 1997;26:185–91.
[10] Qin QH, Mai YW. Thermoelectroelastic Green's function and its application for bimaterial of piezoelectric materials. Arch Appl Mech 1998;68(6):433–44.
[11] Aliabadi MH, Brebbia CA, editors. Advances in boundary element methods for fracture mechanics. Southampton: Computational Mechanics Publications; 1993.
[12] Qin QH. Green's function for thermopiezoelectric materials with holes of various shapes. Arch Appl Mech 1999;69:406–18.
[13] Yin HP, Ehrlacher A. Variational approach of displacement discontinuity method and application to crack problems. Int J Frac 1993;63:135–53.
[14] Qin QH. Green's function and its application for piezoelectric plate with various openings. Arch Appl Mech 1999;69:133–44.
[15] Aliabadi MH, Rooke DP. Numerical fracture mechanics. Southampton: Computational Mechanics Publishers; 1991.